

# Reactions of rare earth acetate hydrates in glycols at high temperatures

M. INOUE, T. NISHIKAWA, H. KOMINAMI, T. INUI

*Department of Energy and Hydrocarbon Chemistry, Graduate School of Engineering, Kyoto University, Yoshida, Kyoto 606-8501, Japan*  
E-mail: inoue@scl.kyoto-u.ac.jp

The reaction of rare earth acetate hydrate in ethylene glycol at 300°C yielded two novel crystalline products, one from La-Gd and the other from Tb-Lu and Y. IR and NMR spectra of these products suggested the presence of both acetate groups and ethylene glycol moieties, and it was concluded that these products are ethylene glycol complexes of rare earth acetate (hydroxide) oxide. On the other hand, the reaction of rare earth acetate hydrate in other glycols such as 1,3-propanediol and 1,4-butanediol yielded rare earth diacetate hydroxide, two morphs of rare earth acetate oxide and rare earth acetate dihydroxide, depending on the ionic size of rare earth element, but the glycol complexes were not formed. In all cases, acetate groups of rare earth acetate were not completely eliminated from the coordination sites of the rare earth element by the reaction in glycols but the reaction in ethylene glycol could liberate the acetate groups more easily than other glycols because of high coordination ability of ethylene glycol. © 2000 Kluwer Academic Publishers

## 1. Introduction

Recently, the present authors reported that the reaction of a stoichiometric mixture of aluminum alkoxide and yttrium acetate hydrate in 1,4-butanediol (1,4-BG) at 300°C (glycothermal reaction) yielded single phase microcrystalline yttrium aluminum garnet (YAG) [1]. The use of 1,4-BG is essential for the formation of crystalline garnet under the glycothermal conditions and when ethylene glycol (EG) was used instead of 1,4-BG, an amorphous product was obtained [2]. Subsequently, the authors found that this method can be applied for the synthesis of series of rare earth (RE) aluminum and gallium garnets [3, 4] and that samarium and europium aluminum garnets, which can not be prepared by any other methods, are also formed by this method [3]. They also reported that the glycothermal reactions of RE acetate hydrates with triethyl phosphate or with niobium pentaethoxide yielded the corresponding RE phosphates or niobates, respectively [5, 6]. In order to elucidate the mechanisms for these reactions, the authors explored the reaction of RE acetate hydrate alone in various glycols and found that several novel crystalline phases are formed by the reaction.

## 2. Experimental procedure

### 2.1. Materials

Hydrate salts of RE acetates were purchased from Wako Pure Chemical Industry. Guaranteed grade glycols (Wako) were used without further purification.

### 2.2. Typical reaction procedure

Yttrium acetate tetrahydrate (4.24 g, 12.5 mmol) was suspended in 88 ml of EG in a test tube serving as autoclave liner, and the test tube was placed in a 200-ml autoclave. An additional 18 ml of EG was placed in the gap between the autoclave wall and the test tube. The autoclave was completely purged with nitrogen, heated to 300°C at a rate of 2.3°C/min, and kept at that temperature for 2 h. After the assembly was cooled to room temperature, the resulting product was washed by repeated cycles of centrifugation and decantation and then dried in air.

### 2.3. Analyses

X-ray powder diffraction (XRD) was measured on a Shimadzu DX-D1 diffractometer using Cu K $\alpha$  radiation and a carbon monochromator. Temperature-programmed XRD experiments were carried out on a vertical goniometer equipped with the sample heating unit in a flow of Ar using Ni filtered Cu K $\alpha$  radiation. The <sup>13</sup>C NMR spectra at 67.8 MHz were obtained on a JEOL GSX-270 spectrometer using the cross polarization (CP) technique. About 4.5 kHz sample spinning at the magic angle (MAS) was used. Infrared (IR) spectra were measured on a Shimadzu IR-430 spectrometer using the usual KBr technique or on a JEOL JIR-7000 FT spectrometer using the diffuse reflectance method. Thermal analyses were performed on a Shimadzu TG-50 thermal analyzer at

a heating rate of 10°C/min in a 40-ml/min flow of dried air.

### 3. Results and discussion

As reported in the previous paper [7, 8], the reactions of RE acetate hydrates in 1,4-BG yielded RE diacetate hydroxide (DAH,  $\text{RE}(\text{OAc})_2(\text{OH})$ ), RE acetate dihydroxide (ADH,  $\text{RE}(\text{OAc})(\text{OH})_2$ ), and two modifications of RE acetate oxide (AOA and AOB,  $\text{RE}(\text{OAc})\text{O}$ ), depending on the ionic radius of the RE elements [7, 8]. The reactions in 1,3-propanediol (1,3-PG) or 1,5-pentanediol showed a product spectrum similar as the reactions in 1,4-BG, although the yields of the ADH phase were smaller as compared with the reaction in 1,4-BG. Results are summarized in Table I.

The reactions in EG gave products completely different from those obtained in 1,4-BG or other glycols. Two types of crystalline products were detected, one for La-Gd and the other for Tb-Lu and Y; hereafter these products will be referred as Phase A and Phase B, respectively. The XRD patterns of the Phase A products are given in Fig. 1 and those of the Phase B products

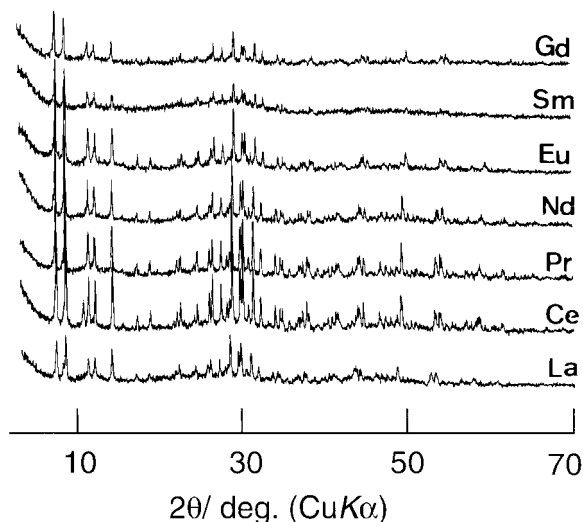


Figure 1 XRD patterns of the Phase A products obtained by the reactions of rare earth (La-Gd) acetates in ethylene glycol at 300°C for 2 h.

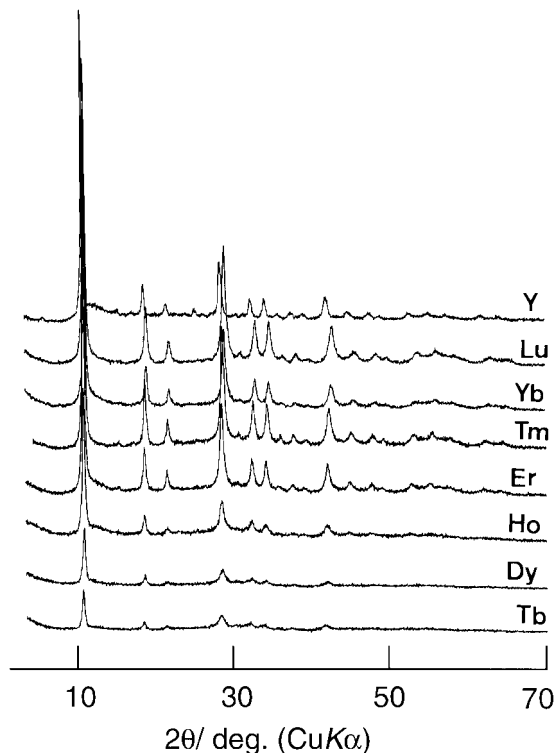


Figure 2 XRD patterns of the Phase B products obtained by the reactions of rare earth (Tb-Lu, and Y) acetates in ethylene glycol at 300°C for 2 h.

are shown in Fig. 2. These results are rather surprising because the glycothermal reaction of the mixtures of aluminum isopropoxide and RE acetates in EG gave amorphous products [2, 3]. As shown in Figs 1 and 2, the products with RE elements near the boundary of the two phases exhibited the XRD peaks with relatively low intensities and therefore these products may be contaminated with the amorphous phase.

To elucidate the effect of the reaction temperature, some of RE acetates were allowed to react in EG at 200°C. The reactions of acetates of Gd and Yb afforded amorphous products, while acetates of Tb and Ho gave poorly crystallized products, whose XRD patterns were similar with that reported by Manabe and Ogawa as a new modification of anhydrous lanthanum acetate [9].

TABLE I Product phases of the reactions of rare earth acetate hydrates in glycols at 300°C for 2 h

Element	Glycol			
	Ethylene Glycol	1,3-Propanediol	1,4-Butanediol	1,5-Pentanediol
La	Phase A	DAH	DAH	DAH
Ce	Phase A	DAH	DAH	—
Pr	Phase A	AOA, (DAH)	AOA, (DAH)	—
Nd	Phase A	AOA	AOA	AOA
Sm	Phase A	AOA	AOA	—
Eu	Phase A	AOA	ADH, (AOA)	—
Gd	Phase A	AOA, (ADH)	ADH, (AOA)	AMM
Tb	Phase B	ADH, AOB	AOA	—
Dy	Phase B	AOA	AOB, (AOA)	AOA
Ho	Phase B	AOB	AOB	—
Er	Phase B	AOB	AOB	—
Tm	Phase B	—	AOB	—
Yb	Phase B	AOB	AOB	Unidentified
Lu	Phase B	—	AOB, AAH	—
Y	Phase B	—	AOB, AAH	AOB

DAH, rare earth diacetate hydroxide,  $\text{RE}(\text{OAc})_2(\text{OH})$ ; AOA and AOB, rare earth acetate oxide ( $\text{RE}(\text{OAc})\text{O}$ ) with two different structures; ADH, rare earth acetate dihydroxide ( $\text{RE}(\text{OAc})(\text{OH})_2$ ); AAH, rare earth acetate anhydride; AMM, acetate monohydrate ( $\text{RE}(\text{OAc})_3 \cdot \text{H}_2\text{O}$ ). Phases shown in parentheses were present in minor quantities.

TABLE II Interconversion of the products obtained by the reaction of rare earth acetate in ethylene glycol and in 1,3-propanediol<sup>a</sup>

Element	Starting Phase <sup>b</sup>	Medium	Product <sup>b</sup>
La	DAH	Ethylene Glycol	Phase A
Nd	AOA	Ethylene Glycol	Phase A
Gd	AOA, (ADH)	Ethylene Glycol	Phase A, Phase B
Tb	ADH, AOB	Ethylene Glycol	Phase B
Er	AOB	Ethylene Glycol	Phase B
Yb	AOB	Ethylene Glycol	Phase B
La	Phase A	1,4-Butanediol	AOA, (Unidentified)
Nd	Phase A	1,4-Butanediol	AOA
Gd	Phase A	1,4-Butanediol	Phase C
Tb	Phase B	1,4-Butanediol	Phase C
Er	Phase B	1,4-Butanediol	Phase C
Yb	Phase B	1,4-Butanediol	Phase C

<sup>a</sup>The air-dried starting material, obtained by the reaction of rare earth acetate in a glycol at 300°C for 2 h, was further treated in another glycol specified in the table at 300°C for 2 h.

<sup>b</sup>DAH, rare earth diacetate hydroxide,  $\text{RE}(\text{OAc})_2(\text{OH})$ : AOA and AOB, rare earth acetate oxide ( $\text{RE}(\text{OAc})\text{O}$ ) with two different structures: ADH, rare earth acetate dihydroxide ( $\text{RE}(\text{OAc})(\text{OH})_2$ ).

However, because of the low crystallinity of these products, further characterization of was not carried out.

The reaction of acetates of La and Pr in EG at 200°C yielded the corresponding DAH phase, although both the products were contaminated with small amounts of unidentified product(s). This result suggests that the Phase A products, at least those obtained from acetates of La and Pr, were formed via the DAH phase. In order to verify this assumption, the products obtained by the reaction of RE acetates in 1,3-PG were further treated in EG at 300°C. The results are summarized in Table II. Irrespective of the starting phases, the products of these reactions were essentially identical with those of the direct reactions of RE acetates in EG, although the Gd species gave a mixture of Phase A and Phase B.

On the other hand, when the Phase A product obtained by the reaction of neodymium acetate in EG was treated in 1,4-BG, Nd(OAc)O (AOA) was obtained. Similar treatment of the Phase A product from lanthanum acetate did not afford the DAH phase, which was the product of the direct reaction of lanthanum acetate in glycols other than EG, but yielded the AOA phase together with a small amount of unidentified crystalline phase(s). The reactions in 1,4-BG of the Phase A product obtained from gadolinium acetate and of all the products with Phase B structure gave another novel crystalline phase. This phase will be called Phase C, whose XRD pattern is shown in Fig. 3. The results mentioned above can be summarized as follows: The products obtained by the reactions of RE acetates in 1,3-PG can be converted to the products formed by the reactions in EG but the reverse reactions take place in limited cases.

Typical IR spectra of Phases A and B are shown in Fig. 4. Both the spectra of Phases A and B showed characteristic bands due to the acetate group and the EG moiety, but apparent difference is that Phase B exhibited sharp bands at  $\sim 3650\text{ cm}^{-1}$  while Phase A did not show these bands. This suggests that Phase B possesses the structural OH group while Phase A does not. A broad band at around  $3400\text{ cm}^{-1}$  observed in Phase B seems to be due to the free OH group of the glycol moiety.

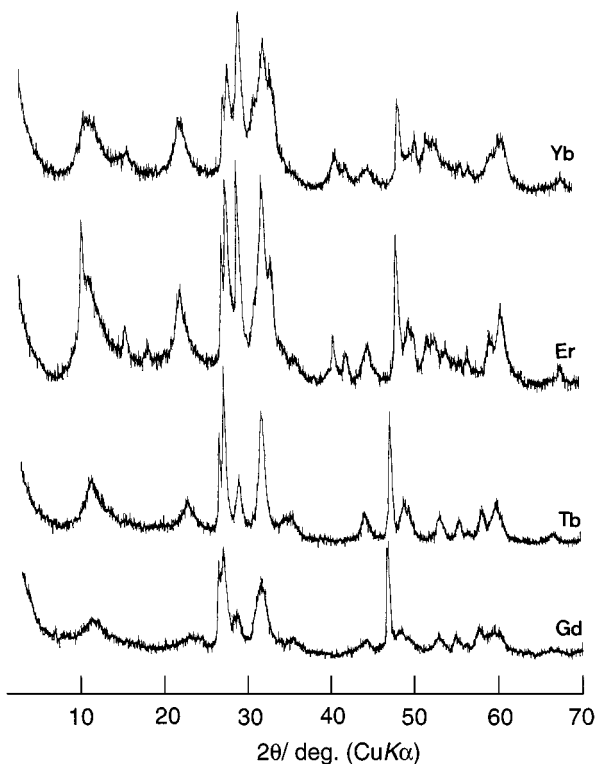


Figure 3 XRD patterns of the Phase C products. For the reaction conditions: See footnote of Table II.

Phase A also exhibited a broad absorption at this region but low intensity of the band suggests that this is due to water or glycol adsorbed on the product surface.

The IR spectra of Phase A showed stretching vibration bands due to the acetate groups at  $1560$  and  $1420\text{ cm}^{-1}$ , and the Phase B products exhibited the corresponding bands at  $1590\text{ cm}^{-1}$  and at around  $1380\text{ cm}^{-1}$ , although unequivocal assignments cannot be made because asymmetric bending mode of the methyl group appears at the same region. These results suggest that the acetate groups in the two phases are in completely different environments. Four types of coordination of acetate groups are generally considered, i.e., monodentate, chelating, bridging, and polymeric [10–12]. They may be characterized by the position and difference between the asymmetric and symmetric vibrations of the carboxylate group and difference between the two vibration frequencies decrease in the following order: monodentate  $\gg$  bridging  $>$  polymeric  $>$  chelating. Phase B exhibited relatively large difference between two bands, which may suggest the presence of the bridging acetate group in this phase.

Liquid EG shows two absorption bands in the  $850\text{--}950\text{ cm}^{-1}$  region. Using normal coordinate analyses, Matsuura and Miyazawa [13] assigned the  $885\text{-cm}^{-1}$  band to the rocking vibration and the  $865\text{-cm}^{-1}$  band to the C–C stretching vibration of gauche isomer coupled with C–O stretching mode. Two other groups reached similar conclusions independently [14, 15]. Miyake prepared two different types of EG (monodentate and bidentate) complexes of cobalt and nickel salts and found that the  $865\text{-cm}^{-1}$  band shifts to ca.  $25\text{ cm}^{-1}$  higher frequency on going from a monodentate to a bidentate complex [16]. Similar shifts were reported

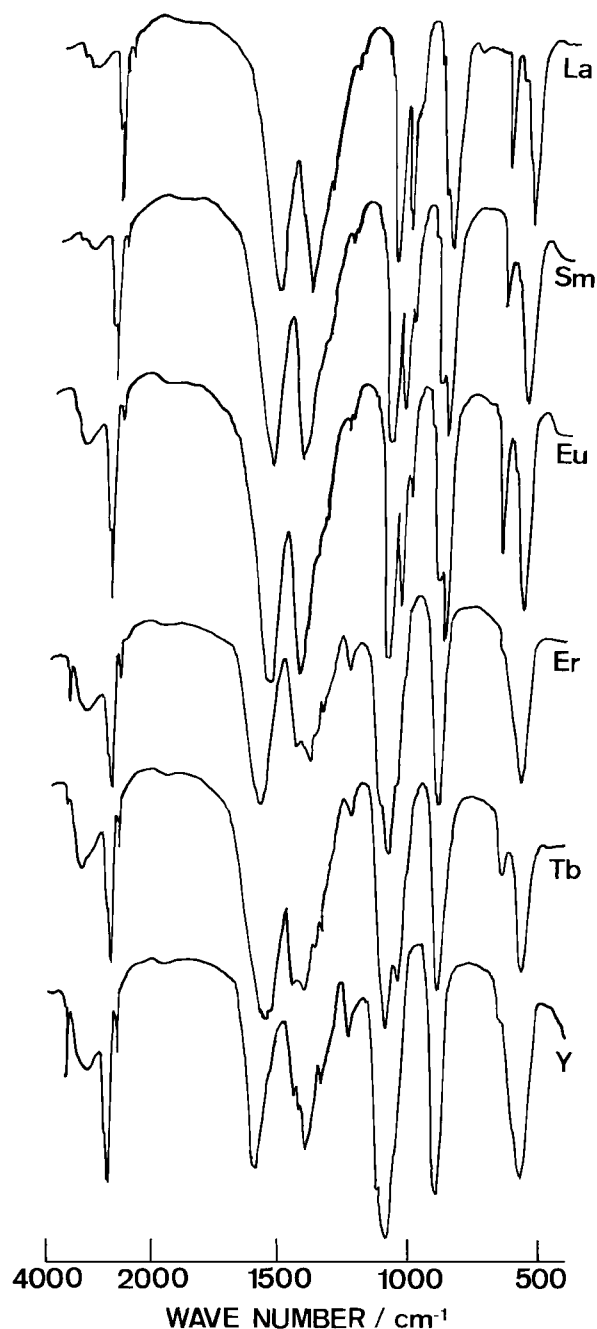


Figure 4 Typical IR spectra of the products obtained by the reactions of rare earth acetates in ethylene glycol at 300°C for 2 h. Spectra were taken by the KBr disk method.

for many other complexes, and some glycolato complexes showed the C–C vibration mode (the 865-cm<sup>-1</sup> band) at higher frequency than the rocking vibration mode (the 885-cm<sup>-1</sup> band). As the 865-cm<sup>-1</sup> bands is mainly due to the C–C vibration mode, shifts to higher frequencies may be attributed to the increase in bond order between two carbon atoms. Actually, shortening of C–C bond in bidentately coordinated EG moiety was reported [17–19]. Although Phase B showed only one absorption band at ~905 cm<sup>-1</sup>, this can be explained by accidental overlap of the 885-cm<sup>-1</sup> band with the 865-cm<sup>-1</sup> band caused by large shift of the latter band to higher frequency, which suggests that EG moiety in Phase B is bidentately bound to a RE ion. The 865-cm<sup>-1</sup> band of Phase A also shifted to higher frequency and it appeared at higher frequency than the 885-cm<sup>-1</sup> band.

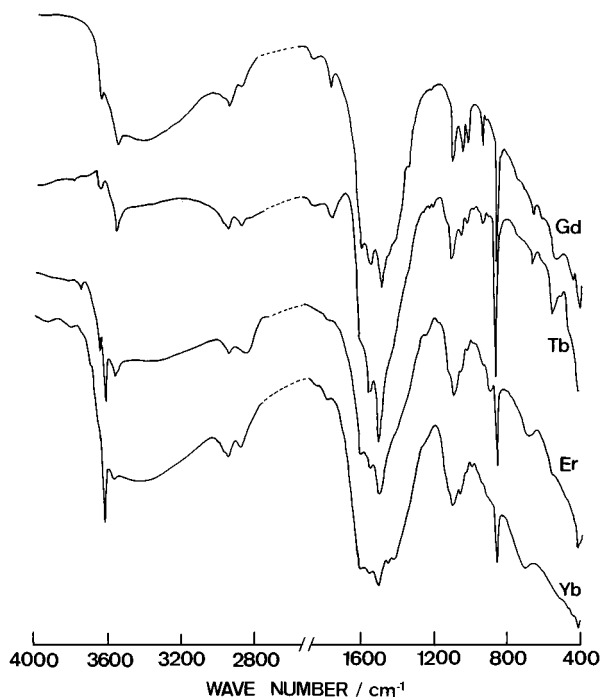


Figure 5 IR spectra of Phase C. Spectra were taken by the diffuse reflectance method.

This suggests that EG moiety in Phase A is strongly coordinated to the RE ion.

The IR spectra of Phase C are shown in Fig. 5. This phase exhibited sharp bands at ca. 3620 cm<sup>-1</sup> due to the stretching vibration of the structural OH groups. The acetate group seems to be present in this phase but asymmetric and symmetric vibration bands were not separated well. This seems to be due to the acetate groups present in several chemical environments and to the chelating form of the acetate group which usually shows a small difference in the frequencies of the two bands. The spectra also indicate that the ethylene glycol moieties present in Phase B were completely expelled by the reaction in 1,4-BG.

The <sup>13</sup>C CPMASNMR spectra of the products obtained by the reaction of lanthanum acetate (Phase A) and yttrium acetate (Phase B) are shown in Fig. 6. For Phase A, peaks at 24.9 and 28.7 ppm are attributed to methyl carbons of acetate ions while peaks at 183.3 and 185.9 ppm are due to carbonyl carbons. These two sets of the peaks suggest that in Phase A the acetate groups are present in at least two different chemical environments. A broad peak at 66.3 ppm is attributed to the methylene carbons of the ethylene glycol moiety. Phase B showed three peaks at 26.2, 69.6, and 178.9 ppm, and these peaks were also attributed to the methyl carbon of the acetate group, the methylene carbons of the EG moiety, and the carbonyl carbon of the acetate group, respectively. The intensity ratio of the peaks suggests that the same number of the methyl carbon and the methylene carbon are present in Phase A, while Phase B contains at least four times larger number of the methylene carbon than that of the methyl carbon.

Thermal analyses of the as-air-dried Phase B products showed that they decomposed through three successive weight decrease processes. The first weight decrease took place at around 140°C with an endothermic

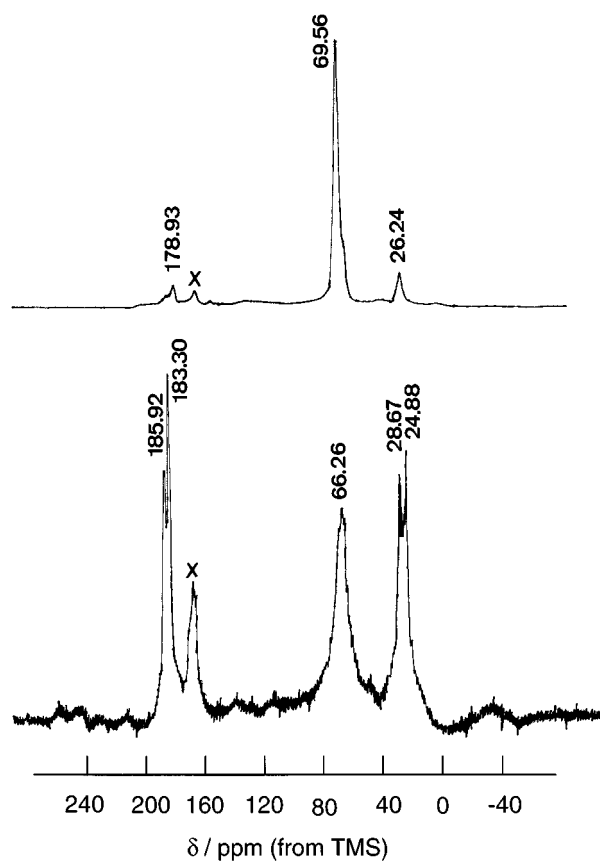


Figure 6  $^{13}\text{C}$  CPMASNMR spectra of Phase A (lower) and Phase B (upper) products obtained by the reactions of lanthanum and yttrium acetates, respectively, in ethylene glycol at  $300^\circ\text{C}$  for 2 h. Peak at  $\delta = 166$  ppm, indicated by X, is due to background.

response in differential thermal analysis (DTA). This weight decrease is due to the desorption of physisorbed glycol molecules. The second weight decrease observed at around  $360^\circ\text{C}$  was associated with a large exothermic peak in DTA and is therefore due to the oxidative degradation of organic moieties. The last weight decrease was observed at  $620\text{--}780^\circ\text{C}$ , and the temperature depended on the RE element. The DTA response also depended on the element; some showed a slight exothermic peak while other showed a slight endothermic one. Total weight loss of this phase was about 30%.

Results for the temperature-programmed XRD experiments were shown in Figs 7 and 8. Phase B became amorphous at  $200\text{--}400^\circ\text{C}$ . From the amorphous phase, RE oxide crystallized at  $\sim 600^\circ\text{C}$ . Because the sample was held at each measurement temperature for 1 h, phase transformation would take place at a lower temperature than that observed in thermal analysis, and therefore the last weight decrease observed in thermal analysis is attributed to the crystallization of RE oxide (exothermic process), which is associated with the loss of surface hydroxyl groups and desorption of carbonate groups (endothermic processes). The DTA response mentioned above may be due to the balance of the heat effects of these two processes.

Phase A showed similar transformation sequence. After the desorption of glycol at around  $140^\circ\text{C}$ , oxidative degradation of organic moieties took place at around  $360^\circ\text{C}$ . The Ce species, however, showed the peak temperature at  $300^\circ\text{C}$ , which can be interpreted by

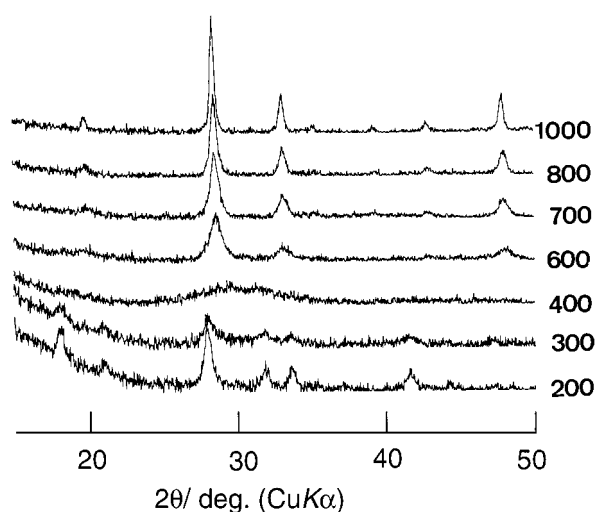


Figure 7 High temperature XRD patterns of the samples derived from a Phase B product obtained by the reaction of thulium acetate in ethylene glycol.

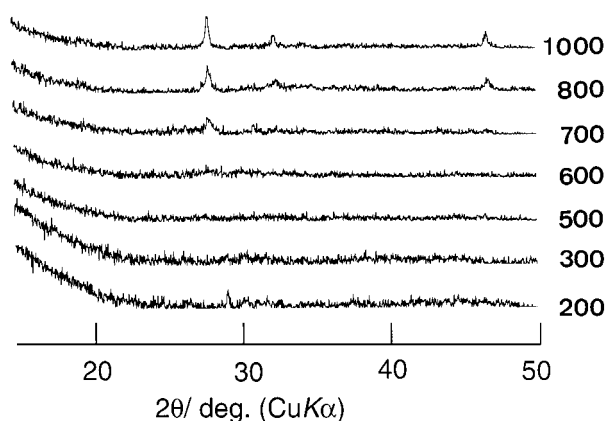


Figure 8 High temperature XRD patterns of the samples derived from a Phase A product obtained by the reaction of gadolinium acetate in ethylene glycol.

the catalytic activity of the Ce species for oxidation. For the La, Ce, Pr, and Eu species, a slight weight decrease was observed at around  $500^\circ\text{C}$ . This weight decrease was associated with an exothermic response in DTA and therefore is attributed to the combustion of carbonaceous material formed by degradation of organic moieties at around  $360^\circ\text{C}$ . The last weight decrease process was observed at  $610\text{--}780^\circ\text{C}$ , which was accompanied by crystallization of RE oxide. Total weight loss of this phase was approximately 30%.

Phase A was much less stable than Phase B and it became amorphous even by heating at  $100^\circ\text{C}$ , as shown in Fig. 8. The oxide phase crystallized at  $700^\circ\text{C}$ . During these temperatures, the carbonate oxide phase ( $\text{RE}_2(\text{CO}_3)\text{O}_2$ ) did not appear. This transformation sequence shows a clear contrast against that of the other RE acetate species such as acetate, acetate hydroxides (DAH and ADH) and acetate oxide (AOA and AOB) [7–10]. These compounds transform into carbonate oxide ( $\text{RE}_2(\text{CO}_3)\text{O}_2$ ) before the final transformation into oxide. One possible explanation for the difference in the thermal transformation sequence is that the acetate groups of the other RE acetate species decomposed into acetone remaining carbonate ion in the coordination

TABLE III Elemental analysis

Element	Calculated			Found		
	C	H	Ignition loss	C	H	Ignition loss
$\text{RE}_2\text{O}(\text{OAc})_2(\text{OCH}_2\text{CH}_2\text{O})$						
La	15.27	2.14	31.97	13.92	2.15	31.0
Ce	15.19	2.12	30.81	7.24	1.08	32.79
Pr	15.14	2.12	30.71	14.98	2.32	33.70
Nd	14.93	2.09	30.28	13.58	2.15	33.27
Sm	14.56	2.04	29.53	12.72	2.30	30.24
Eu	14.47	2.02	29.34	14.16	2.17	32.57
Gd	14.17	1.98	28.73	12.68	2.24	34.29
$\text{RE}_2\text{O}(\text{OCH}_2\text{CH}_2\text{OH})_2(\text{OAc})(\text{OH})$						
Tb	13.55	2.65	31.23	12.93	2.21	25.74
Dy	13.37	2.62	30.82	11.72	1.92	27.48
Ho	13.25	2.59	30.54	11.68	2.06	30.93
Er	13.13	2.57	30.29	13.64	2.28	27.17
Tm	13.05	2.56	30.10	13.89	2.42	32.49
Yb	12.86	2.52	29.66	13.29	2.29	31.22
Lu	12.78	2.50	29.46	13.91	2.25	29.39
Y	18.38	3.60	42.39	15.33	2.81	41.79

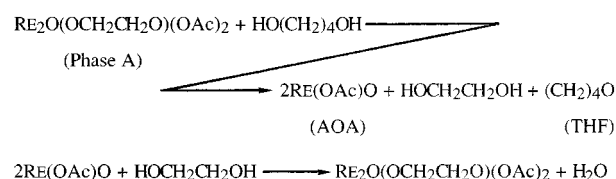
site of the RE ion, while the presence of the glycol moiety in the present products enables the acetate groups to form volatile esters by the reaction with the glycol moieties and to be eliminated without the formation of carbonate species. An alternative explanation is that the transformation of the acetate oxide phase into the carbonate oxide phase is a topotactic process and that the crystal structure of the precursor phases may not be adequate for the crystallization of the carbonate oxide phase.

Results for elemental analyses and ignition loss determined by thermal analysis are summarized in Table III. On the basis of the results mentioned above, the empirical formulas of Phase A and Phase B are tentatively assigned as  $\text{RE}_2\text{O}(\text{OCH}_2\text{CH}_2\text{O})(\text{OAc})_2$  and  $\text{RE}_2\text{O}(\text{OCH}_2\text{CH}_2\text{OH})_2(\text{OAc})(\text{OH})$ , respectively, although the agreement between calculated and observed C and H contents was relatively poor because of the possible presence of the amorphous phase.

Thermal analysis of Phase C showed two weight decrease processes. The first one occurred at 300–400°C which was associated with an exothermic peak in DTA. The second one took place at 550–650°C and the peak temperature depended on the RE element. This weight decrease was accompanied by an endothermic response in DTA. Although the IR spectra of the intermediate phase indicated the presence of the carbonate group (1510 and 860  $\text{cm}^{-1}$ ), the XRD pattern of this phase did not agree with that of the carbonate oxide phase but was similar to the oxide phase; therefore, the second weight decrease was attributed to the desorption of carbonate species adsorbed on the particles of the oxide phase. Total weight decrease was ca. 16%, which suggests that Phase C has an empirical formula of  $\text{RE}_2\text{O}_2(\text{OAc})(\text{OH})$ .

The interconversion between the products obtained in EG and other glycols (Table III) can be explained by the proposed empirical formula. Because the OAc/RE ratio in Phase B is 1/2, this phase cannot be converted to  $\text{RE}(\text{OAc})\text{O}$  (OAc/RE = 1), while the reverse reaction can take place. On the other hand, Phase A has

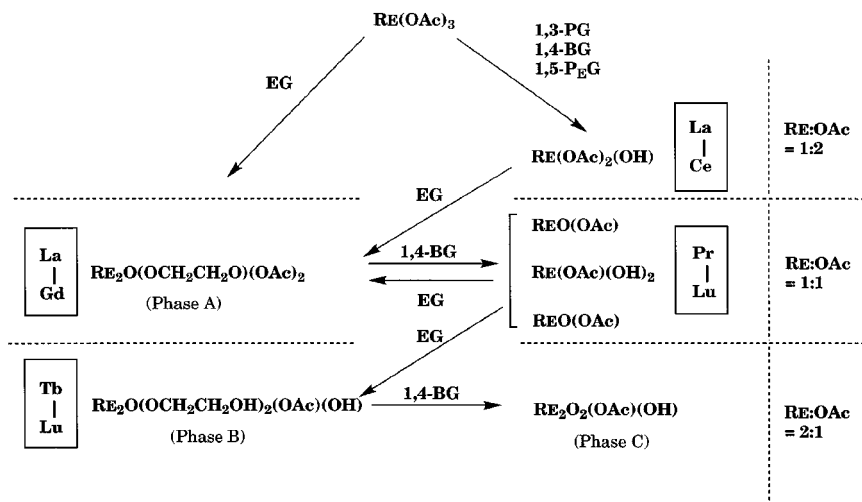
OAc/RE = 1; therefore, it cannot be converted to the DAH phase (OAc/RE = 2) and interconversion between Phase A and  $\text{RE}(\text{OAc})\text{O}$  occurred: The reaction equations can be described as follows



The driving force of these two reactions can be attributed to the removal of low boiling point products (THF and water) from the reaction system by evaporation into the gas phase. Formation of tetrahydrofuran (THF) in the reaction of aluminum alkoxide in 1,4-BG was demonstrated and it was explained that cleavage of the C–O bond in 1,4-BG moiety was facilitated by the intramolecular participation of the hydroxyl group [20].

The interconversion of the products obtained in EG and in other glycols is schematically shown in Scheme 1. Although the scheme is slightly oversimplified, it can explain the essence of the present work. Under the glycothermal conditions only a part of the acetate groups were eliminated from the coordination sites of RE ions. With the decrease in the ionic radius of the RE element, cleavage of the bonds between the acetate groups and RE ions proceeds more easily. When the reaction in EG is compared with the reaction in 1,4-BG or other glycols, the reaction in EG facilitates the removal of the acetate groups from the coordination sites of RE ions. This seems to be due to the high coordination ability of EG molecules.

This paper demonstrated that in the glycothermal reaction of RE acetate alone, acetate groups are not completely expelled from the coordination sites of the RE ions. On the other hand, in the glycothermal



Scheme 1 Interconversion of the products.

synthesis of RE aluminum or gallium garnets by the reaction of RE acetate with aluminum alkoxide or gallium acetylacetonate, all the acetate groups of RE acetate were eliminated from the coordination sites of the RE ions [1, 3, 4]. Therefore, aluminum alkoxide, gallium acetylacetonate, or some species derived therefrom under the glycothermal reaction must have coordination abilities higher than EG and facilitate the cleavage of the bonds between the RE ion and the acetate groups. Thermal decomposition of the glycol moieties of aluminum or gallium glycoxide, formed by ester exchange between the alkoxide or acetylacetonate with glycol, yields O-anion species ( $>Al-O^-$  or  $>Ga-O^-$ ) which seem to be the most probable species having high ability for mediating the cleavage between the RE ions and the acetate groups in the glycothermal synthesis of RE garnets.

#### 4. Conclusions

Two novel EG complexes of RE acetate (hydroxide) oxide were obtained by the reaction of RE acetate hydrate in EG at 300°C; one obtained from La-Gd had a empirical formula of  $RE_2O(OCH_2CH_2O)(OAc)_2$  and the other obtained from Tb-Lu and Y,  $RE_2O(OCH_2CH_2OH)_2(OAc)(OH)$ . The reaction of RE acetate hydrate in other glycols such as 1,3-propanediol and 1,4-butanediol did not yield the glycol complexes but gave RE diacetate hydroxide, two morphs of acetate oxide, and acetate dihydroxide, depending on the ionic size of the RE element. The ratio of acetate/RE in the product obtained in EG was always smaller than that in the product obtained in other glycols, which can be attributed to the high coordination ability of EG.

#### Acknowledgements

The present work was partly supported by a Grant-in-Aid for Scientific Research on Priority Areas "New

Development of Rare Earth Complexes" No. 06241243 and No. 07230251 from The Ministry of Education, Science and Culture, Japan.

#### References

1. M. INOUE, H. OTSU, H. KOMINAMI and T. INUI, *J. Amer. Ceram. Soc.* **74** (1991) 1452.
2. *Idem.*, *Nippon Kagakukai-shi.* (1991) 1358.
3. *Idem.*, *J. Alloys Comp.* **226** (1995) 146.
4. M. INOUE, H. OTSU, H. KOMINAMI, T. NAKAMURA and T. INUI, *J. Mater. Sci. Lett.* **14** (1995) 1303.
5. M. INOUE, T. NAKAMURA, H. OTSU, H. KOMINAMI and T. INUI, *Nippon Kagakukai-shi* (1993) 612.
6. H. KOMINAMI, M. INOUE and T. INUI, *Catal. Today* **16** (1993) 309.
7. M. INOUE, H. KOMINAMI and T. INUI, *Nippon Kagakukai-shi* (1991) 1254.
8. H. KOMINAMI, M. INOUE and T. INUI, *ibid.* (1993) 605.
9. K. MANABE and M. OGAWA, *ibid.* (1979) 1012.
10. D. G. KARRAKER, *J. Inorg. Nucl. Chem.* **31** (1969) 2815.
11. K. NAKAMOTO, "Infrared and Raman Spectra of Inorganic and Coordination Compounds" (Wiley, New York, 1978) p. 232.
12. F. RIBOT, P. TOLENDI and C. SANCHEZ, *Inorg. Chim. Acta* **185** (1991) 239.
13. H. MATSUURA and T. MIYAZAWA, *Bull. Chem. Soc. Jpn.* **40** (1967) 85.
14. K. KRISHNAN and R. S. KRISHNAN, *Proc. Indian Acad. Sci.* **A64** (1966) 111.
15. W. SAWODNY, K. NIEDENZU and J. W. DAWSON, *Spectrochim. Acta Part A.* **23A** (1967) 799.
16. A. MIYAKE, *Bull. Chem. Soc. Jpn.* **32** (1959) 381.
17. D. BRIGHT, G. H. W. MIBURU and M. R. TRUTER, *J. Chem. Soc., A* (1971) 1582.
18. E. A. SCHROEDER, J. SCHERLE and R. G. HAZELL, *Acta Crystallogr., Ser. B; Struct. Crystallogr. Cryst. Chem.* **B31** (1975) 531.
19. M. C. CRUICKSHANK and L. S. DENT GLASSER, *Acta Crystallogr.* **C41** (1985) 1014.
20. M. INOUE, H. KOMINAMI and T. INUI, *J. Chem. Soc. Dalton Trans.* (1991) 3331.

Received 6 October 1997

and accepted 30 September 1999